

Optimization of Microelectrode Design for Cortical Recording Based on Thermal Noise Considerations

Scott F. Lempka, *Student Member, IEEE*, Matthew D. Johnson, *Student Member, IEEE*, David W. Barnett, *Member, IEEE*, Michael A. Moffitt, Kevin J. Otto, *Member, IEEE*, Daryl R. Kipke, *Member IEEE* and Cameron C. McIntyre

Abstract—Intracortical microelectrode recordings of neural activity show great promise as control signals for neuroprosthetic applications. However, faithful, consistent recording of single unit spiking activity with chronically implanted silicon-substrate microelectrode arrays has proven difficult. Many approaches seek to enhance the long-term performance of microelectrode arrays by, for example, increasing electrode biocompatibility, decreasing electrode impedance, or improving electrode interface properties through application of small voltage pulses. The purpose of this study was to use computational models to optimize the design of microelectrodes. We coupled detailed models of the neural source signal, silicon-substrate microelectrodes, and thermal noise to define the electrode contact size that maximized the signal-to-noise ratio (SNR). Model analysis combined a multi-compartment cable model of a layer V cortical pyramidal neuron with a 3D finite element model of the head and microelectrode to define the amplitude and time course of the recorded signal. A spatially-lumped impedance model was parameterized with *in vitro* and *in vivo* spectroscopy data and used to define thermal noise as a function of electrode contact size. Our results suggest that intracortical microelectrodes with a contact size of $\sim 380 \mu\text{m}^2$ will provide an increased SNR *in vivo* and improve the long-term recording capabilities of silicon-substrate microelectrode arrays.

I. INTRODUCTION

BRAIN machine interfaces (BMI) represent an emerging area of neurotechnology with wide ranging clinical

This work was supported by a grant from the Ohio Biomedical Research and Technology Transfer Partnership.

S.F. Lempka is with the Department of Biomedical Engineering, Cleveland Clinic Foundation, Cleveland, OH 44195 USA and the Department of Biomedical Engineering, Case Western Reserve University, Cleveland, OH 44106 USA (corresponding author phone: 216-445-3291; fax: 216-445-9198; e-mail: sfl5@case.edu).

M.D. Johnson is with the Department of Biomedical Engineering, University of Michigan, Ann Arbor, MI 48109 USA (e-mail: mdjzz@umich.edu).

D.W. Barnett is with the Department of Biomedical Engineering, Saint Louis University, St. Louis, MO 63103 USA (e-mail: barnettd@slu.edu).

M.A. Moffitt was with the Cleveland Clinic Foundation, Cleveland, OH 44195 USA. He is now with Advanced Bionics, Sylmar, CA 91342 USA (e-mail: mmoffitt@advancedbionics.com).

K.J. Otto was with the University of Michigan, Ann Arbor, MI 48109 USA. He is now with the Department of Biological Sciences, Purdue University, West Lafayette, IN 47907 USA (e-mail: kotto@purdue.edu).

D.R. Kipke is with the Department of Biomedical Engineering, University of Michigan, Ann Arbor, MI 48109 USA (e-mail: dkipke@umich.edu).

C.C. McIntyre is with the Department of Biomedical Engineering, Cleveland Clinic Foundation, Cleveland, OH, 44195 USA and the Department of Biomedical Engineering, Case Western Reserve University, Cleveland, OH 44106 USA (e-mail: mcintyc@ccf.org).

applications. However, BMIs have yet to achieve large-scale clinical acceptance because of the infancy of the technology and limitations in the long-term recording capabilities of the microelectrode arrays. We hypothesize that it is possible to improve the long-term recording capabilities of these arrays by optimizing the electrode design with accurate computational models of cortical recording. We have previously developed detailed computer models of single unit extracellular recording with silicon-substrate microelectrodes [1]. However, our original models ignored the effects of noise on the recorded waveforms.

Thermal noise is thought to be the dominant noise source encountered when performing cortical microelectrode recordings largely in part to the high impedance of the microelectrodes. Thermal noise is due to the thermal electron agitation in a conductor and can be estimated using the Johnson-Nyquist formula [2, 3]. To estimate the spectral density of the thermal noise, both the transfer function of the combined filter stages and the real (i.e. resistive) component of the system impedance over the recording bandwidth are needed. Because thermal noise is directly related to the electrode impedance, it is also related to the surface area of the electrode contact (small contact \rightarrow high impedance \rightarrow high noise). In addition, the surface area of the contact impacts the signal amplitude recorded from the neuron (large contact \rightarrow low amplitude).

The focus of this project was to integrate the effects of thermal noise into our computer model of cortical microelectrode recording and define a contact surface area that maximized the signal-to-noise ratio (SNR). We combined thermal noise estimates from *in vitro* and *in vivo* impedance measurements of silicon-substrate microelectrodes with neural recordings generated in our model system. This analysis was performed for a range of electrode contact sizes to determine the design that provided the highest SNR. The results of this study may prove useful in improving the design and long-term recording capabilities of current microelectrode technology.

II. METHODS

We expanded our previously-published model of microelectrode cortical recording [1] to account for the effects of thermal noise. A previously-published impedance model [4] was used to fit *in vitro* and *in vivo* impedance spectroscopy data to a parametric equation describing the system impedance as a function of frequency. This impedance data was then used to estimate the thermal noise for various electrode contact designs. SNR was evaluated as

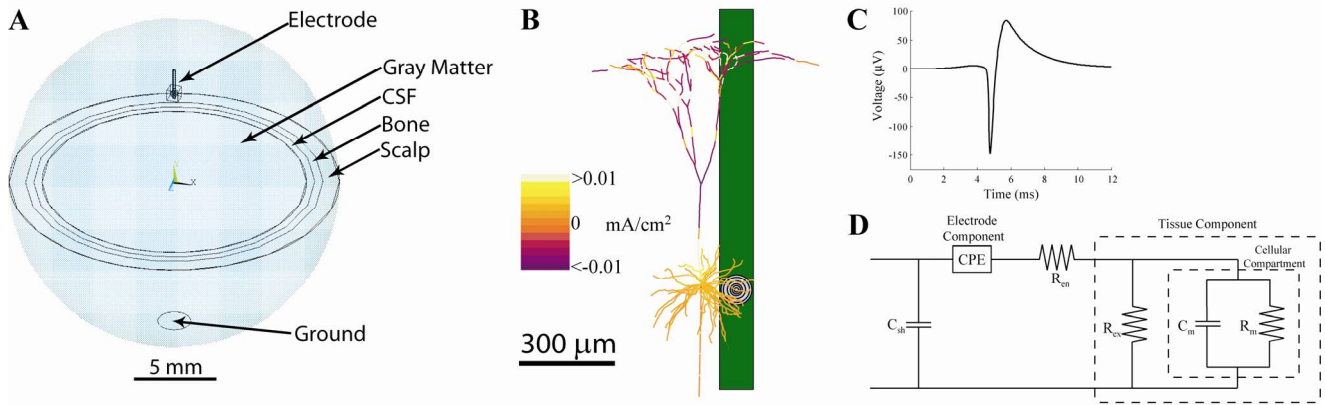


Fig. 1. (A) Finite-element model of a rat head with explicit representation of a silicon-substrate microelectrode. (B) Close-up image of the neural source model next to the recording electrode model. (C) Simulated extracellular recording from the coupled field-neuron model. (D) Spatially-lumped *in vivo* impedance model used to estimate thermal noise

a function of the electrode contact surface area using the appropriate estimates for thermal noise and signal amplitude.

A. Electrode Impedance Spectroscopy

Electrode impedance spectroscopy (EIS) measurements were taken using a 25 mV sine wave at 11 frequencies ranging from 100 Hz to 10 kHz [4]. *In vitro* impedance measurements were made using electrodes of various contact sizes. Test probes with platinum sites of 50, 177, 380, 1520, and 2830 μm^2 were fabricated and tested.

In vivo EIS measurements were made on multiple silicon-substrate microelectrode arrays in motor cortex of two Sprague-Dawley rats (250-300 g, implanted for 97 and 338 days). EIS data were used to estimate the encapsulation, cellular, and extracellular components of the impedance model described below. Surgical procedures for these implants have been described previously [4].

B. Impedance Model

A spatially-lumped impedance model was used to estimate recording parameters and is shown in Fig. 1D [4]. In the model, the electrode-electrolyte interface is represented by a constant phase element (CPE) with a magnitude scaling factor (K) and a phase factor (α) defined for $0 \leq \alpha \leq 1$.

$$Z_{CPE} = \frac{K}{(j\omega)^\alpha} \quad (1)$$

The CPE accounts for the pseudo-capacitive behavior of the electrode-electrolyte interface and is based on empirical data [5]. The CPE is connected in series with an encapsulation resistance, R_{en} , which represents the electrode encapsulation formed as part of the body's immune response [6]. The extracellular space is represented by R_{ex} and the cellular tissue component is represented by a parallel combination of a specific membrane conductance (g_m) and capacitance (C_m) that is multiplied by a membrane area scaling term (A_m). The values of g_m and C_m are 0.3 mS/cm² and 1 $\mu\text{F}/\text{cm}^2$, respectively [7]. The shunt capacitance of the electrode shank, represented by C_{sh} , was found to be < 10 pF. A non-linear regression algorithm was used to estimate model parameters from the complex impedance spectroscopy measurements [4].

C. Cortical Recording Model

The computational model of cortical recording used in this study included two major components: an electrical volume conductor and an electrical field source model [1]. The electrical volume conductor consisted of a finite element model (FEM) of a rat head with a silicon-substrate microelectrode inserted in the cortex (Fig. 1A). The electrical source model consisted of a multi-compartment cable model of a layer V cortical pyramidal neuron (Fig. 1B) [1, 8].

1) *Electrical Volume Conductor Model*: The volume conductor model contained four concentric spheres representing the brain, cerebrospinal fluid (CSF), skull, and scalp. The FEM also included explicit representation of a silicon-substrate microelectrode. The electrode shank had a width of 107 μm , length of 2000 μm , and a thickness of 15 μm . The microelectrode contacts were circular with radii of 4, 7.5, 11, 22, or 30 μm corresponding to approximate surface areas of 50, 177, 380, 1520, or 2830 μm^2 , respectively. The volume conductor models were assumed to be purely resistive and were generated in Ansys v8.0 (Ansys, Inc., Canonsburg, PA) [1].

2) *Electrical Source Model*: A preexisting neuron model of a cat visual cortex layer V pyramidal cell [8] was modified according to [1] and simulated in NEURON v5.8 [9].

3) *Model Coupling*: The neuron model was positioned with its cell body 50 μm from the electrode contact and the coordinates of each compartment were integrated into the FEM (Fig 1b). A reciprocity-based technique was used to estimate the neural signal recorded at the microelectrode contact using a single FEM solution (Fig. 1C) [1].

D. Noise Model

Average model parameters for the electrode component of the impedance model (K and α) for the given contact sizes were determined using the EIS measurements of the test probes in 0.1 M phosphate buffered saline (PBS) (pH 7.4). Average model parameters for the tissue component (R_{ex} , R_{en} , and A_m) of the impedance model described above were

estimated from *in vivo* EIS measurements of rats with chronically implanted microelectrode arrays. The parameters R_{ex} , R_{en} , and A_m were assumed to be independent of electrode contact size. For a given contact size, the average parameter values for both the electrode and tissue components were combined and used to derive an expression for recording impedance as a function of frequency based on the impedance model. The impedance expression was then used to estimate the thermal noise spectral density using the Johnson-Nyquist formula:

$$S_v(\omega) = 2kT \operatorname{Re}(Z(\omega)) \quad (2)$$

Where k represents the Boltzmann constant and T is the absolute temperature. The equation above is true for any passive, reciprocal network and can be used to describe the noise voltage across two arbitrary terminals, such as the working and ground electrodes [10]. As evident by the impedance model (Fig. 1D), at low frequencies the recording impedance becomes extremely high due to the capacitive nature of the electrode-electrolyte interface. At high frequencies, the recording impedance becomes small due to the electrode shunt capacitance and the capacitive nature of both the electrode-electrolyte interface and the membranes of cells in the surrounding media. However, the noise bandwidth is eventually bandpass filtered by the data acquisition system. A typical recording bandwidth for cortical microelectrode single-unit recordings is 450-5000 Hz [4, 11]. The effects of the bandpass filtering can be accounted for using the following equation:

$$S(\omega) = S_v(\omega) |H_{sig}(\omega)|^2, \quad (3)$$

where H_{sig} represents the transfer function of the combined filter stages.

After estimating the noise spectral density, the noise variance was predicted by integration. Because the noise is zero-mean, integration of the autospectral density leads directly to the noise variance.

For the neural recording model, a sampling rate of 40 kHz and a simulation time of 12 ms were used. The noise spectrum, $S(\omega)$, was evaluated over the frequency range of 0 to 20 kHz, corresponding to the frequency range for the discrete Fourier transform of the simulated neural recording. H_{sig} consisted of a two-pole low-pass Butterworth filter with a cutoff frequency of 5 kHz and a two-pole high-pass Butterworth filter with a cutoff frequency of 450 Hz in order to simulate a typical recording bandwidth of 450-5000 Hz. The temperature in (2) was set equal to a physiological temperature of 310 K. All of the numerical methods described above were performed using Matlab 7.0 (Mathworks, Natick, MA).

E. SNR Analysis

The simulated neural recordings and noise spectral densities were used to estimate the SNR for each contact size. The SNR for a given contact size was defined as the peak-to-peak amplitude of the simulated neural recording divided by twice the standard deviation of the noise determined from the noise spectral density [12].

III. RESULTS

A. Impedance Parameter Estimation

In vitro EIS measurements were performed in 0.1 M PBS to define the electrode parameters, K and α [4] (Table 1).

TABLE I
AVERAGE ELECTRODE PARAMETERS

Contact Radius (μm)	K	α
4	6.65×10^9	0.79
7.5	5.74×10^9	0.82
11	1.11×10^9	0.82
22	6.67×10^8	0.88
30	4.21×10^8	0.85

In vivo EIS measurements were taken from rats with chronically implanted microelectrode arrays to estimate the tissue parameters of the impedance model (R_{en} , R_{ex} , and A_m) [4]. Data was obtained from two different microelectrode arrays and 26 different contact sites. The average values for R_{en} , R_{ex} , and A_m were 357 ± 44 k Ω , 433 ± 163 k Ω , and 207 ± 134 μm^2 , respectively.

B. Noise Estimation and SNR Analysis

The average tissue component parameters (R_{en} , R_{ex} , and A_m) were combined with average electrode parameters (K and α) and used to estimate the total recording impedance as function of frequency. The impedance spectrum was then used to estimate the thermal noise spectral density from (2). Filtering effects were approximated from the transfer function of the band-pass filter according to (3). Integration of the noise spectral density led directly to the noise variance.

Using this method, noise levels with standard deviations of 7.97, 7.46, 6.74, 6.40, and 6.42 μV were estimated for contacts surface areas of 50, 177, 380, 1520, and 2830 μm^2 , respectively (Fig. 2B). These values show the expected result of decreasing noise levels with increasing contact surface areas. Recorded signal amplitudes were estimated using a computational model of cortical recording. Model analysis was performed and peak-to-peak signal amplitudes of 177, 175, 171, 156, and 142 μV were returned for contact surface areas of 50, 177, 380, 1520, and 2830 μm^2 , respectively (Fig. 2B). These noise levels and signal amplitudes corresponded to signal-to-noise ratios of 11.1, 11.7, 12.7, 12.2, and 11.1 for contact surface areas of 50, 177, 380, 1520, and 2830 μm^2 , respectively (Fig. 2C).

IV. DISCUSSION

This study utilized detailed computer models of cortical recording with silicon-substrate microelectrodes and experimental measurements of electrode impedance to define theoretically optimal microelectrode contact designs based on thermal noise considerations. When optimizing the SNR for intracortical microelectrode recording there is a trade-off between decreasing the contact surface area to increase signal amplitude and increasing the contact surface area to minimize thermal noise. For the contact sizes

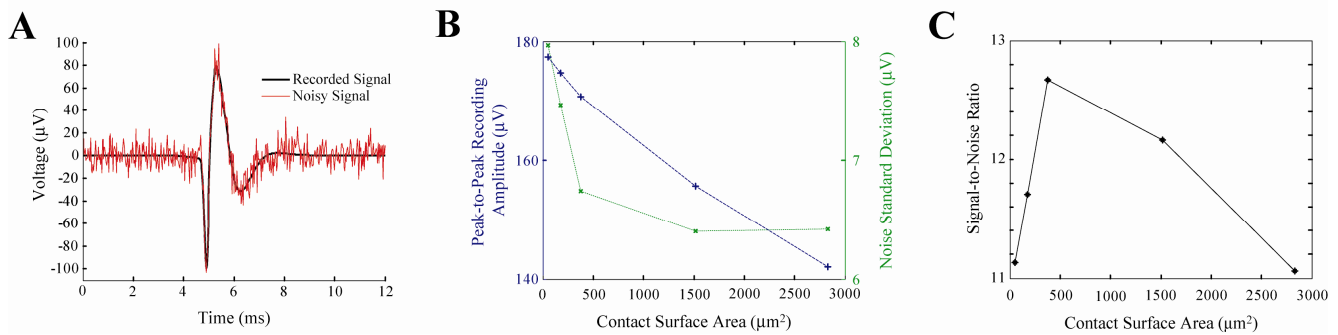


Fig. 2. (A) Simulated extracellular neural recording for a contact surface area of $50\mu\text{m}^2$ shown with and without the estimated thermal noise. (B) Peak-to-peak signal amplitudes and thermal noise levels as a function of contact surface area. (C) Signal-to-noise ratio as a function of contact surface area.

examined, the results of this study suggest that the optimal contact size is $\sim 380\mu\text{m}^2$ (Fig. 2C).

Contact surface areas less than $380\mu\text{m}^2$, only provided a small increase in signal amplitude that was overshadowed by a substantial increase in thermal noise due to the increased electrode impedance (Fig. 2B). As the contact surface area increased above $380\mu\text{m}^2$, the decrease in thermal noise was small but there was a substantial decrease in signal amplitude, resulting in a lower SNR (Fig. 2B).

The results of this study provide theoretical guidelines to improve the design of cortical microelectrodes; however, the model systems have a number of limitations that should be recognized. First, the experimental EIS data used to parameterize the electrode impedance model often suffers from substantial variability, resulting from various degrees of encapsulation. This variability limits our ability to assign definitive parameter values. We are currently addressing this limitation by increasing our experimental recording sample size and performing a battery of parameter sensitivity studies to address the impact of model parameter variability. Modifications to the recording model will be made to include an explicit representation of the electrode-electrolyte interface and capacitive effects of the electrode and biological media. *In vivo* recording experiments will also be performed in order to validate the model results and to examine the effect of contact size on tissue parameters in the impedance model.

The thermal noise levels predicted using the electrode impedance spectroscopy data and the Johnson-Nyquist formula are similar to but lower than noise levels encountered experimentally [11]. This observation shows the importance of modeling other noise sources when optimizing microelectrode design. Therefore, in future work a second major source of recording noise, biological noise from neurons in the surrounding media, will be considered in the electrode optimization.

In spite of the various limitations, the model analysis provides new insight into the optimization of microelectrodes for intracortical recording. The model results show that a contact size of $\sim 380\mu\text{m}$ provides a good balance between increased recording amplitude and decreased thermal noise. Intracortical microelectrodes with recording sites of this size will result in a higher SNR and

may improve the long-term recording capabilities of microelectrode arrays used in brain-machine interfacing.

ACKNOWLEDGMENTS

The authors would like to thank the Center for Neural Communication Technology for fabricating and assembling the probes, as well as Harry Wiggins and Justin Williams for helpful discussion.

REFERENCES

- [1] M.A. Moffitt and C.C. McIntyre, "Model-based analysis of cortical recording with silicon microelectrodes," *Clin. Neurophysiol.*, vol. 116, no. 9, pp. 2240-2250, Sep. 2005.
- [2] J.B. Johnson, "Thermal agitation of electricity in conductors," *Phys. Rev.*, vol. 32, pp 97-109, July 1928.
- [3] H. Nyquist, "Thermal agitation of electric charge in conductors," *Phys. Rev.*, vol. 32, pp 110-113, July 1928.
- [4] K. Otto, M. Johnson, and D.R. Kipke, "Voltage pulses change neural interface properties and improve unit recordings with chronically implanted microelectrodes," *IEEE Trans. on Biomed. Eng.*, vol. 53, no. 2, pp. 333-340, Feb. 2006.
- [5] E.T. McAdams, A. Lackermeier, J.A. McLaughlin, and D. Macken, "The linear and non-linear electrical properties of the electrode-electrolyte interface," *Biosens. Bioelectron.*, vol. 10, pp. 67-74, 1995.
- [6] W.M. Grill and J.T. Mortimer, "Electrical properties of implant encapsulation tissue," *Ann. Biomed. Eng.*, vol. 22, pp. 23-33, 1994.
- [7] J.R. Buitengeweg, W.L.C. Rutten, W.P.A. Willems, and J.W. van Nieuwkastele, "Measurement of sealing resistance of cell-electrode interfaces in neuronal cultures using impedance spectroscopy," *Med. Biol. Eng. Comput.*, vol. 36, no. 5, pp. 630-637, Sep. 1998.
- [8] Z.F. Mainen, J. Joerges, J.R. Huguenard, and T.J. Sejnowski, "A model of spike initiation in neocortical pyramidal neurons," *Neuron*, vol. 15, no. 6, pp. 1427-1439, Dec. 1995.
- [9] M.L. Hines and N.T. Carnevale, "The NEURON simulation environment," *Neural Comput.*, vol. 9, no. 6, pp. 1179-1209, Aug. 1997.
- [10] A. Papoulis, *Probability, Random Variables, and Stochastic Processes*. New York: McGraw-Hill, 1984, ch. 10.
- [11] R.J. Vetter, J.C. Williams, J.F. Hetke, E.A. Numamaker, D.R. Kipke, "Chronic neural recording using silicon-substrate microelectrode arrays implanted in cerebral cortex," *IEEE Trans. on Biomed. Eng.*, vol. 51, no. 6, pp. 896-904, June 2004.
- [12] C.T. Nordhausen, E.M. Maynard, R.A. Normann, "Single unit recording capabilities of a 100 microelectrode array," *Brain Res.*, vol. 726, pp. 129-140, July 1996.